Available online at www.sciencedirect.com
ScienceDirect
European Journal of Mechanics B/Fluids 27 (2008) 632–641

Nonlinear convective flows in multilayer fluid system

Ilya B. Simanovskii [a,*], Antonio Viviani [b], Jean-Claude Legros [c]

[a] *Department of Mathematics, Technion – Israel Institute of Technology, 32000 Haifa, Israel*
[b] *Seconda Universita di Napoli (SUN), Dipartimento di Ingegneria Aerospaziale e Meccanica (DIAM), via Roma 29, 81031 Aversa, Italy*
[c] *Universite Libre de Bruxelles, Service de Chimie Physique EP, CP165-62, 50 Av. F.D. Roosevelt 1050, Brussels, Belgium*

Received 3 April 2007; received in revised form 2 October 2007; accepted 11 November 2007

Available online 28 November 2007

Abstract

The nonlinear thermocapillary and buoyant-thermocapillary flows in a three-layer system, filling a closed cavity and subjected to a temperature gradient directed along the interfaces, are investigated. The nonlinear simulations of convective regimes are performed by the finite-difference method. The process of transition of unicell structures into multicell structures is studied.

Keywords: Convective flows; Interfaces; Instabilities; Multilayer systems

1. Introduction

Prediction of the fluids behavior under microgravity conditions is an important problem in space engineering. Experiments in space revealed the dominant role of the thermocapillary convection in the microgravity fluid dynamics. The case when the system has only one interface between different fluids has been studied analytically and numerically in many works (see, for example, the monograph [1]). Convection in the system with one interface and one free surface was considered in [2].

The interfacial convection in multilayer systems is a widespread phenomenon that is of great importance in numerous branches of technology (for a review, see [3]). The most well-known modern engineering technique that requires an investigation of convection in multilayer systems is the liquid encapsulation crystal growth technique [4,5] used in space labs missions. Another important problem is the droplet–droplet coalescence, where Marangoni convection in the interdroplet film can considerably affect the coalescence time during extraction [6]. Simultaneous interaction of interfaces with their bulk phases and with each other was studied for heating from below and from above [7,8], as well as in the case of the horizontal temperature gradients [9–12].

Thermocapillary flows in multilayer systems with periodic boundary conditions on lateral boundaries, subjected to a temperature gradient directed along the interfaces, have been studied in [13]. It was found that the traveling waves move in the direction of the temperature gradient. For sufficiently large values of the Marangoni number, pulsating traveling waves changing their shape and intensity, have been observed. The nonlinear buoyant-thermocapillary flows

* Corresponding author.
E-mail address: yuri11@zahav.net.il (I.B. Simanovskii).

0997-7546/$ – see front matter
doi:10.1016/j.euromechflu.2007.11.003

in three-layer systems with periodic boundary conditions have been studied in [14]. Transitions between different convective regimes have been investigated. The general diagram of flow regimes on the plane the Marangoni number–the Grashof number, has been constructed.

Let us emphasize, that the theoretical predictions obtained for infinite layers, cannot be automatically applied to flows in closed cavities, because of several reasons. First, in the case of periodic boundary conditions one observes waves generated by a *convective* instability of parallel flow, while for the observation of waves in a closed cavity a *global* instability is needed [15]. Also, it should be taken into account, that in the presence of rigid lateral walls the basic flow is not parallel anymore. The lateral walls act as a stationary finite-amplitude perturbation that can produce *steady* multicellular flow in the part of the cavity and in the whole cavity [15].

The nonlinear thermocapillary convective flows in a closed cavity filled by a *symmetric* three-layer system (the exterior layers had the same thermophysical properties), have been investigated in [16]. Nonlinear regimes of steady and oscillatory convective flows have been studied; during the oscillatory process the number of vortices in the layers was changed.

Evidently, that symmetric systems cannot exist under the action of gravity because of the Rayleigh–Taylor instability. The nonlinear simulations of buoyant-thermocapillary flows in a *closed cavity* filled by three *different* viscous fluids with a temperature gradient directed along the interfaces, have been performed in [17]. Generally, long unicell structures have been obtained in each fluid layer. Examples of buoyant three-layer flows in a closed cavities have been presented in [14] (for a review, see [3]).

In the present work, nonlinear thermocapillary and buoyant-thermocapillary flows in asymmetric three-layer system silicone oil 1-ethylene glycol–fluorinert FC75 filling the closed cavity, subjected to a temperature gradient directed along the interfaces, are investigated. It is found that at sufficiently large values of the Marangoni number, the long unicell vortices turn into the multicell structures. The specific type of nonlinear oscillations is obtained.

The paper is organized as follows. In Section 2, the mathematical formulation of the problem is presented. The nonlinear approach is described in Section 3. Nonlinear simulations of finite-amplitude convective regimes are considered in Section 4. Section 5 contains some concluding remarks.

2. General equations and boundary conditions

We consider a system of three horizontal layers of immiscible viscous fluids with different physical properties (see Fig. 1). The thicknesses of the layers are a_m, $m = 1, 2, 3$. The m-th fluid has density ρ_m, kinematic viscosity ν_m, dynamic viscosity $\eta_m = \rho_m \nu_m$, thermal diffusivity χ_m, heat conductivity κ_m and thermal expansion coefficient β_m.

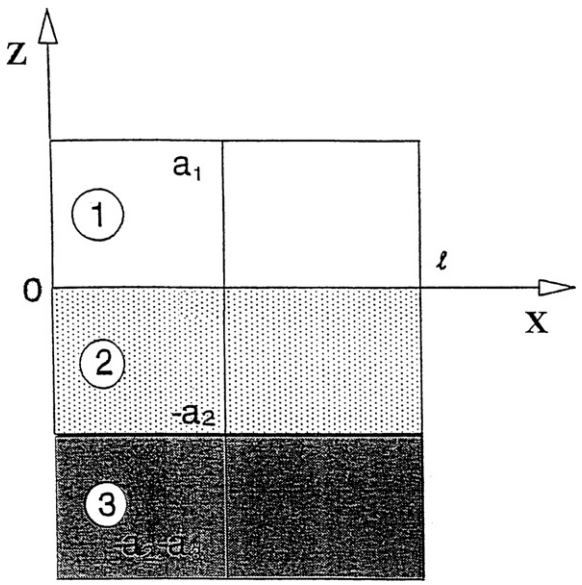

Fig. 1. Geometrical configuration of the three-layer system and coordinate axes.

The system is bounded from above and from below by two rigid plates, $z = a_1$ and $z = -a_2 - a_3$. A constant temperature gradient is imposed in the direction of the axis x: $T_1(x, y, a_1, t) = T_3(x, y, -a_2 - a_3, t) = -Ax + const$, $A > 0$. The surface tension coefficients on the upper and lower interfaces, σ and σ_*, are linear functions of temperature T: $\sigma = \sigma_0 - \alpha T$, $\sigma_* = \sigma_{*0} - \alpha_* T$, where $\alpha > 0$ and $\alpha_* > 0$.

Let us define

$$\rho = \frac{\rho_1}{\rho_2}, \quad \nu = \frac{\nu_1}{\nu_2}, \quad \eta = \frac{\eta_1}{\eta_2} = \rho\nu, \quad \chi = \frac{\chi_1}{\chi_2}, \quad \kappa = \frac{\kappa_1}{\kappa_2}, \quad \beta = \frac{\beta_1}{\beta_2}, \quad a = \frac{a_2}{a_1},$$
$$\rho_* = \frac{\rho_1}{\rho_3}, \quad \nu_* = \frac{\nu_1}{\nu_3}, \quad \eta_* = \frac{\eta_1}{\eta_3} = \rho_*\nu_*, \quad \chi_* = \frac{\chi_1}{\chi_3}, \quad \kappa_* = \frac{\kappa_1}{\kappa_3}, \quad \beta_* = \frac{\beta_1}{\beta_3}, \quad a_* = \frac{a_3}{a_1}, \quad \bar{\alpha} = \frac{\alpha_*}{\alpha}.$$

As the units of length, time, velocity, pressure and temperature we use a_1, a_1^2/ν_1, ν_1/a_1, $\rho_1\nu_1^2/a_1^2$ and Aa_1. The complete nonlinear equations governing convection are then written in the following dimensionless form:

$$\frac{\partial \mathbf{v}_m}{\partial t} + (\mathbf{v}_m \cdot \nabla)\mathbf{v}_m = -e_m \nabla p_m + c_m \Delta \mathbf{v}_m + b_m G T_m \mathbf{e}, \tag{1}$$
$$\frac{\partial T_m}{\partial t} + \mathbf{v}_m \cdot \nabla T_m = \frac{d_m}{P} \Delta T_m, \tag{2}$$
$$\nabla \mathbf{v}_m = 0, \quad m = 1, 2, 3. \tag{3}$$

Here $\mathbf{v_m} = (v_{mx}, v_{my}, v_{mz})$ is the velocity vector, T_m is the temperature and p_m is the pressure in the m-th fluid; $\mathbf{e}$ is the unit vector of the axis z; $e_1 = c_1 = b_1 = d_1 = 1$, $e_2 = \rho$, $c_2 = 1/\nu$, $b_2 = 1/\beta$, $d_2 = 1/\chi$, $e_3 = \rho_*$, $c_3 = 1/\nu_*$, $b_3 = 1/\beta_*$, $d_3 = 1/\chi_*$; $\Delta = \nabla^2$, $G = g\beta_1 A a_1^4/\nu_1^2$ is the Grashof number, and $P = \nu_1/\chi_1$ is the Prandtl number determined by the parameters of the top layer.

The boundary conditions on the isothermic rigid boundaries are:

$$\mathbf{v}_1 = 0, \quad T_1 = T_0 - x \quad \text{at } z = 1, \tag{4}$$
$$\mathbf{v}_3 = 0, \quad T_3 = T_0 - x \quad \text{at } z = -a - a_*, \tag{5}$$

where T_0 is constant.

The conditions on the rigid lateral boundaries, which are assumed to be thermally insulated, are

$$x = 0, L: \quad v_m = 0, \quad \frac{\partial T_m}{\partial x} = 0, \quad m = 1, 2, 3. \tag{6}$$

Let us discuss the boundary conditions at the interface between two fluids. It is known that the interfacial deformation is a non-Boussinesq effect [18]. Indeed, the Boussinesq approximation is based on the assumption $\epsilon_\beta = \beta_1\theta \ll 1$, $G = \mathrm{O}(1)$, therefore the Galileo number $Ga = G/\epsilon_\beta = ga_1^3/\nu_1^2 \gg 1$. However, the balance of normal stresses on the interface shows that the interface deformation is proportional to $1/Ga\delta$, where $\delta = \rho^{-1} - 1$ (see [1]). Because $1/Ga\delta = \epsilon_\beta/G\delta$ is small unless $\delta \ll 1$, we come to the conclusion that in the framework of the Boussinesq approximation the interfacial deformation has to be neglected, if the densities of the fluids are not close to each other. The case of close densities is not considered in the present paper. Thus, we assume that the interfaces between fluids are flat and situated at $z = 0$ and $z = -a$, and put the following system of boundary conditions:

at $z = 0$

$$\frac{\partial v_{1x}}{\partial z} - \eta^{-1}\frac{\partial v_{2x}}{\partial z} - \frac{M}{P}\frac{\partial T_1}{\partial x} = 0, \qquad \frac{\partial v_{1y}}{\partial z} - \eta^{-1}\frac{\partial v_{2y}}{\partial z} - \frac{M}{P}\frac{\partial T_1}{\partial y} = 0, \tag{7}$$
$$v_{1x} = v_{2x}, \quad v_{1y} = v_{2y}, \quad v_{1z} = v_{2z} = 0, \tag{8}$$
$$T_1 = T_2, \tag{9}$$
$$\frac{\partial T_1}{\partial z} = \kappa^{-1}\frac{\partial T_2}{\partial z}; \tag{10}$$

at $z = -a$

$$\eta^{-1}\frac{\partial v_{2x}}{\partial z} - \eta_*^{-1}\frac{\partial v_{3x}}{\partial z} - \frac{\bar{\alpha}M}{P}\frac{\partial T_3}{\partial x} = 0, \qquad \eta^{-1}\frac{\partial v_{2y}}{\partial z} - \eta_*^{-1}\frac{\partial v_{3y}}{\partial z} - \frac{\bar{\alpha}M}{P}\frac{\partial T_3}{\partial y} = 0, \tag{11}$$
$$v_{2x} = v_{3x}, \quad v_{2y} = v_{3y}, \quad v_{2z} = v_{3z} = 0, \tag{12}$$

$$T_2 = T_3, \tag{13}$$

$$\kappa^{-1}\frac{\partial T_2}{\partial z} = \kappa_*^{-1}\frac{\partial T_3}{\partial z}. \tag{14}$$

Here $M = \alpha A a_1^2/\eta_1\chi_1$ is the Marangoni number.

3. Nonlinear approach

In order to investigate the flow regimes generated by the convective instabilities, we perform nonlinear simulations of two-dimensional flows [$v_{my} = 0$ ($m = 1, 2, 3$); the fields of physical variables do not depend on y]. In this case, we can introduce the stream function ψ_m and the vorticity ϕ_m,

$$v_{m,x} = \frac{\partial \psi_m}{\partial z}, \qquad v_{m,z} = -\frac{\partial \psi_m}{\partial x},$$

$$\phi_m = \frac{\partial v_{m,z}}{\partial x} - \frac{\partial v_{m,x}}{\partial z} \quad (m = 1, 2, 3)$$

and rewrite Eqs. (1)–(3) in the following form:

$$\frac{\partial \phi_m}{\partial t} + \frac{\partial \psi_m}{\partial z}\frac{\partial \phi_m}{\partial x} - \frac{\partial \psi_m}{\partial x}\frac{\partial \phi_m}{\partial z} = c_m \Delta\phi_m + b_m G\frac{\partial T_m}{\partial x}, \tag{15}$$

$$\Delta\psi_m = -\phi_m, \tag{16}$$

$$\frac{\partial T_m}{\partial t} + \frac{\partial \psi_m}{\partial z}\frac{\partial T_m}{\partial x} - \frac{\partial \psi_m}{\partial x}\frac{\partial T_m}{\partial z} = \frac{d_m}{P}\Delta T_m \quad (m = 1, 2, 3). \tag{17}$$

Coefficients b_m, c_m and d_m have been defined in Section 2. At the interfaces normal components of velocity vanish and the continuity conditions for tangential components of velocity, viscous stresses, temperatures, and heat fluxes also apply:

$$z = 0: \quad \psi_1 = \psi_2 = 0, \quad \frac{\partial \psi_1}{\partial z} = \frac{\partial \psi_2}{\partial z}, \quad T_1 = T_2, \tag{18}$$

$$\frac{\partial T_1}{\partial z} = \frac{1}{\kappa}\frac{\partial T_2}{\partial z}, \qquad \frac{\partial^2 \psi_1}{\partial z^2} = \frac{1}{\eta}\frac{\partial^2 \psi_2}{\partial z^2} + \frac{M}{P}\frac{\partial T_1}{\partial x}, \tag{19}$$

$$z = -a: \quad \psi_2 = \psi_3 = 0, \quad \frac{\partial \psi_2}{\partial z} = \frac{\partial \psi_3}{\partial z}, \quad T_2 = T_3, \tag{20}$$

$$\frac{1}{\kappa}\frac{\partial T_2}{\partial z} = \frac{1}{\kappa_*}\frac{\partial T_3}{\partial z}, \qquad \frac{1}{\eta}\frac{\partial^2 \psi_2}{\partial z^2} = \frac{1}{\eta_*}\frac{\partial^2 \psi_3}{\partial z^2} + \frac{\tilde{\alpha} M}{P}\frac{\partial T_2}{\partial x}. \tag{21}$$

On the horizontal solid plates the boundary conditions read:

$$z = 1: \quad \psi_1 = \frac{\partial \psi_1}{\partial z} = 0, \quad T_1 = T_0 - x, \tag{22}$$

$$z = -a - a_*: \quad \psi_3 = \frac{\partial \psi_3}{\partial z} = 0, \quad T_3 = T_0 - x, \tag{23}$$

where T_0 is constant.

The calculations were performed in a finite region $0 \leqslant x \leqslant L$, $-a \leqslant z \leqslant 1$ with the following boundary conditions corresponding to rigid heat-insulated lateral boundaries:

$$x = 0, L: \quad \psi_m = \frac{\partial \psi_m}{\partial x} = \frac{\partial T_m}{\partial x} = 0. \tag{24}$$

The boundary value problem was solved by the finite-difference method. Equations were solved using the explicit scheme, on a rectangular uniform mesh 168×56. The Poisson equations were solved by the iterative Liebman successive over-relaxation method on each time step: the accuracy of the solution was 10^{-5}. The details of the numerical method can be found in the book by Simanovskii and Nepomnyashchy [1].

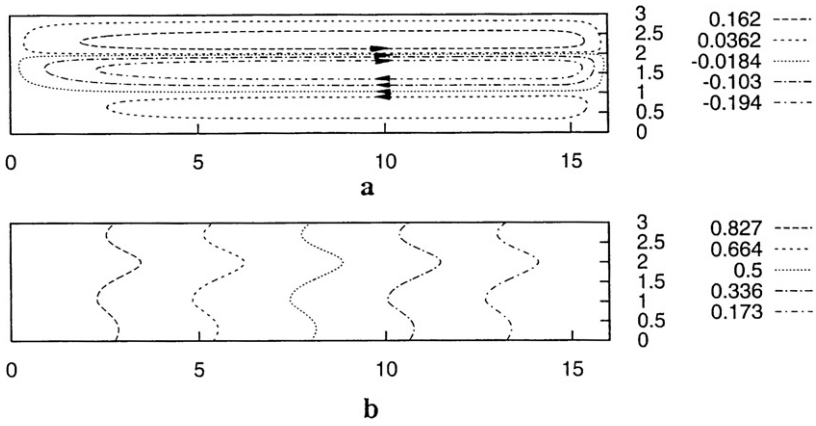

Fig. 2. Snapshots of (a) streamlines and (b) isotherms for the thermocapillary steady flow ($M = 27\,000$, $G = 0$, $L = 16$).

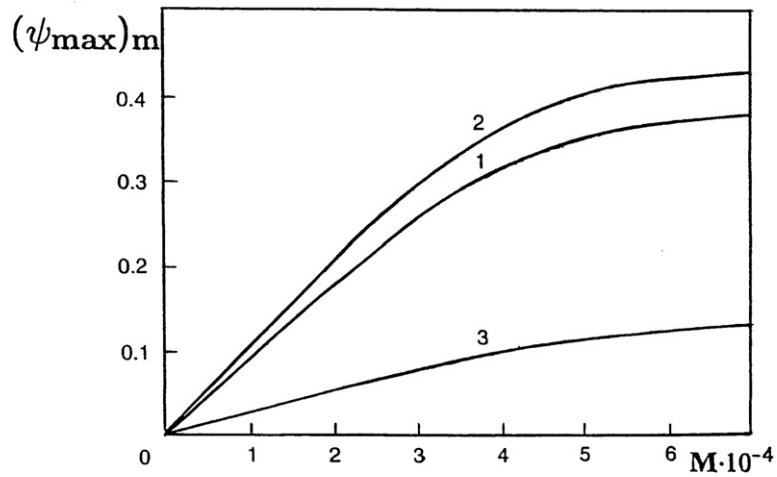

Fig. 3. Dependence of $(\psi_{\max})_m$ ($m = 1, 2, 3$) on M for the thermocapillary steady flow ($G = 0$, $L = 16$).

4. Numerical results

Below we describe results of computations of the nonlinear boundary value problem for the system silicone oil 1-ethylene glycol–fluorinert FC75 with the following set of parameters: $\nu = 0.065$, $\nu_* = 1.251$, $\eta = 0.048$, $\eta_* = 0.580$, $\kappa = 0.390$, $\kappa_* = 1.589$, $\chi = 0.742$, $\chi_* = 2.090$, $\beta = 2.16$, $\beta_* = 0.957$, $\bar{\alpha} = 0.228$, $P = 13.9$. The ratios of the layers thicknesses have been chosen $a = a_* = 1$. Simulations have been performed for $L = 16$ and $L = 32$.

4.1. The case of thermocapillary flows ($M \neq 0$, $G = 0$)

We shall start our analysis by the consideration of the thermocapillary flows ($M \neq 0$, $G = 0$). Let us take $L = 16$.

Even for small values of the Marangoni number ($M \neq 0$) the mechanical equilibrium state is impossible and a steady motion takes place in the system. The streamlines and isotherms for the definite value of the Marangoni number are presented in Fig. 2. One can see that in the central part of the cavity the flow is nearly parallel. Along the upper interface, the fluids move from the hot wall to the cold wall and along the lower interface, the fluids move in the opposite direction. The flow fields in different layers are coupled by viscous stresses. Near the lateral walls the fluid may move both upwards and downwards.

With the increase of the Marangoni number the intensity of the flow near the cold wall becomes higher than that near the hot wall. The finite-amplitude curves show that with the increase of M, the intensity of the motion grows (see Fig. 3). At the larger values of M ($M \geqslant 92000$), the steady state becomes unstable and the transient process takes

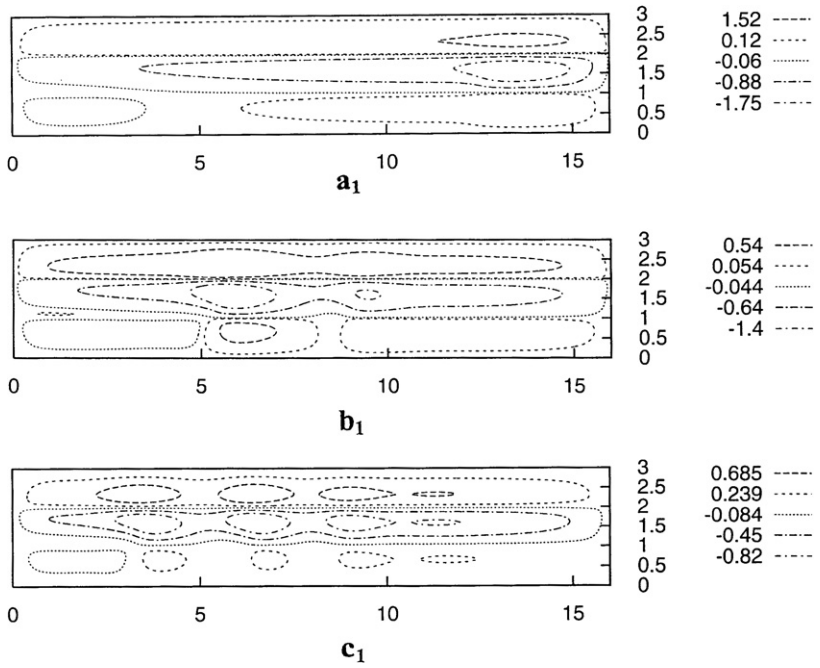

Fig. 4. Snapshots of (a_1)–(c_1) streamlines for the thermocapillary flow at different moments of time ($M = 216\,000$, $G = 0$, $L = 16$).

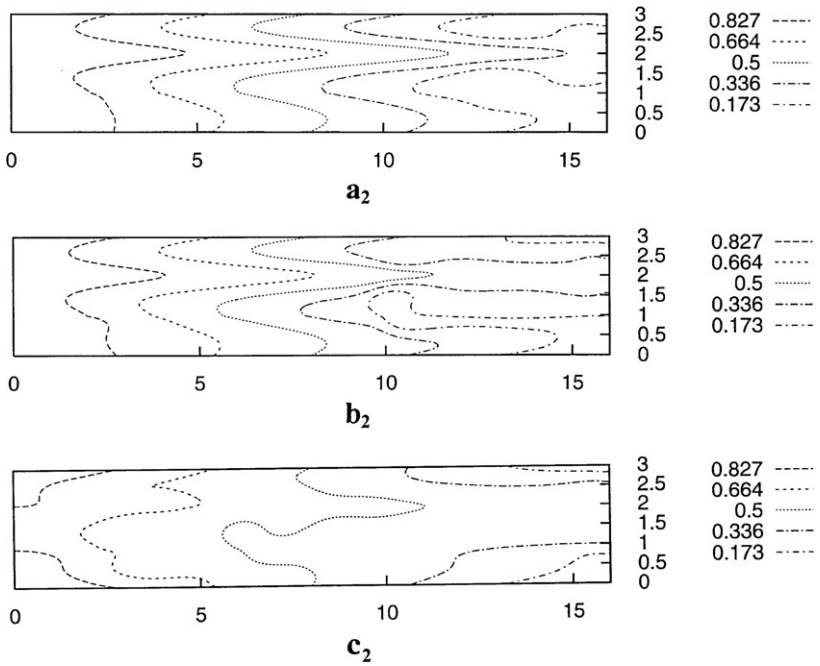

Fig. 5. Snapshots of (a_2)–(c_2) isotherms for the thermocapillary flow at different moments of time ($M = 216\,000$, $G = 0$, $L = 16$).

place in the system (see Figs. 4, 5). The vortices move in the direction of the temperature gradient (Fig. 4(b_1)) and the unicell structure turns into the *multicell* structure in each fluid layer (Fig. 4(c_1)).

For $L = 32$, the transient process of the unicell structure into the multicell structure is presented in Fig. 6. The vortices move from the cold end to the hot end (Fig. 6(b)–(c)). Finally, the oscillatory multicell structure fills in practice all the volume (Fig. 6(d)–(e)). The vortices change their form and intensity during the oscillatory process.

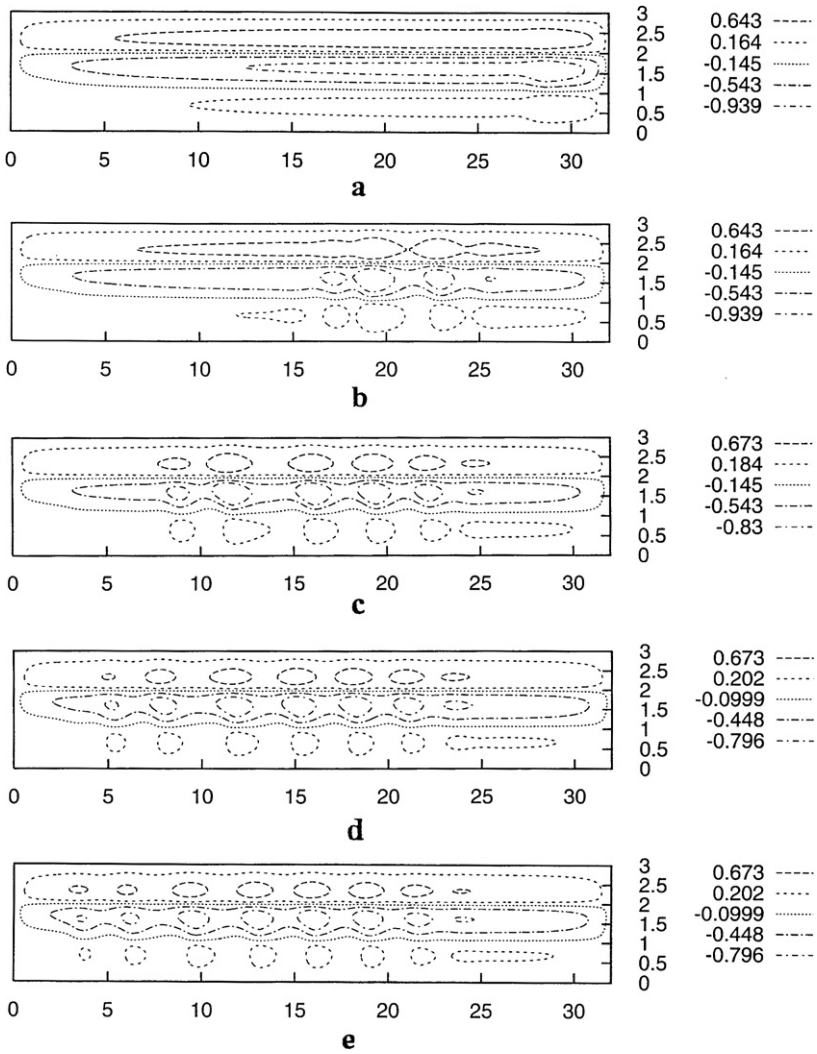

Fig. 6. Snapshots of (a)–(e) streamlines for the thermocapillary flow at different moments of time ($M = 216\,000$, $G = 0$, $L = 32$).

4.2. The case of buoyant-thermocapillary flows ($G \neq 0$, $M \neq 0$)

Let us consider the joint action of buoyancy and the thermocapillary effect. Under the conditions of the experiment, when the geometric configuration of the system is fixed while the temperature difference θ is changed, the Marangoni number M and the Grashof number G are proportional. We define the inverse dynamic Bond number

$$K = \frac{M}{GP} = \frac{\alpha}{g\beta_1\rho_1 a_1^2}.$$

The simulations have been performed for $K = 1.016$ ($L = 16$) and $K = 4.063$ ($L = 32$).

Let us remind that in the case of "short" cavities ($L \leqslant 10$) only unicell structures have been obtained in each fluid layer [17]. We take the cavity with $L = 16$. In the case of buoyant-thermocapillary flows, the stationary flow is essentially asymmetric with respect to the reflection $x \to L - x$ (see Fig. 7). Three of the most intensive vortices are produced mainly by buoyancy (the fluids go upward near the hot wall and go downward near the cold wall). These vortices are separated by vortices rotating in the opposite direction, which are supported by the thermocapillary effect. The finite-amplitude curves for the steady flow are presented in Fig. 8. One can see that depending on G, the most intensive motion may be achieved in different layers. At the larger values of G ($G \geqslant 6500$), the steady motion

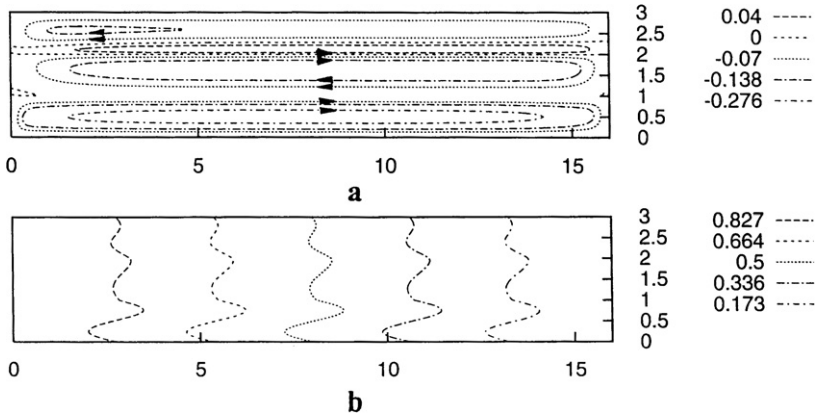

Fig. 7. Snapshot of (a) streamlines and (b) isotherms for the buoyant-thermocapillary steady flow ($G = 1700$, $M = 24\,000$, $L = 16$).

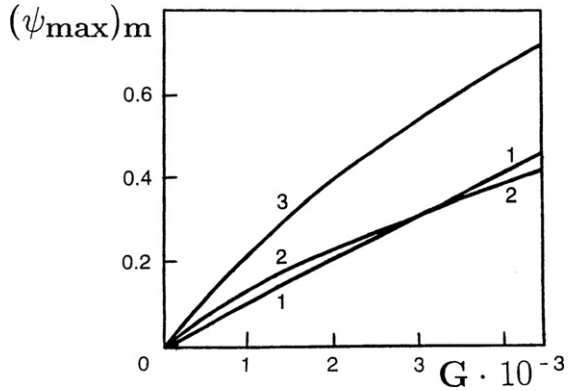

Fig. 8. Dependence of $(\psi_{\max})_m$ $(m = 1, 2, 3)$ on G for the buoyant-thermocapillary steady flow ($K = 1.016$).

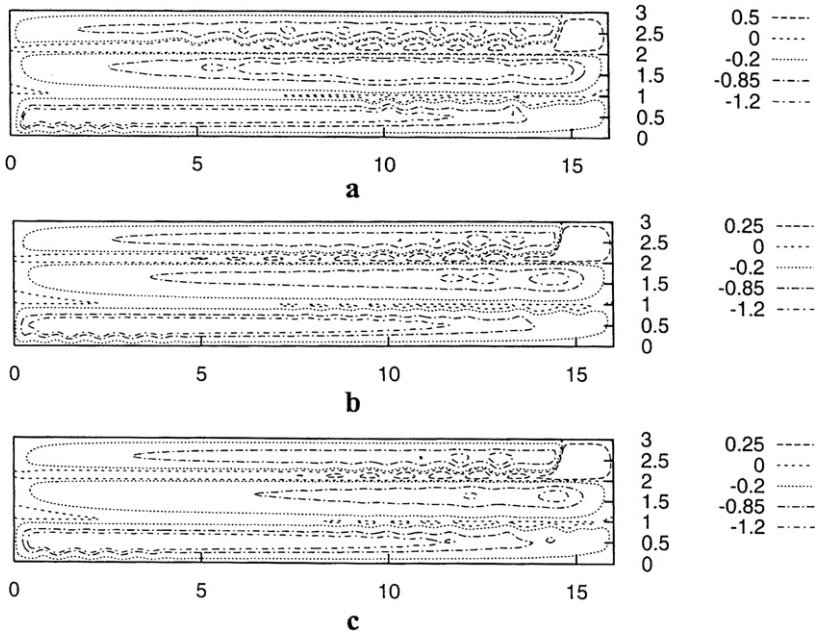

Fig. 9. Fields of (a)–(c) streamlines for the buoyant-thermocapillary oscillatory motion at different moments of time ($G = 15300$, $M = 216\,000$, $L = 16$).

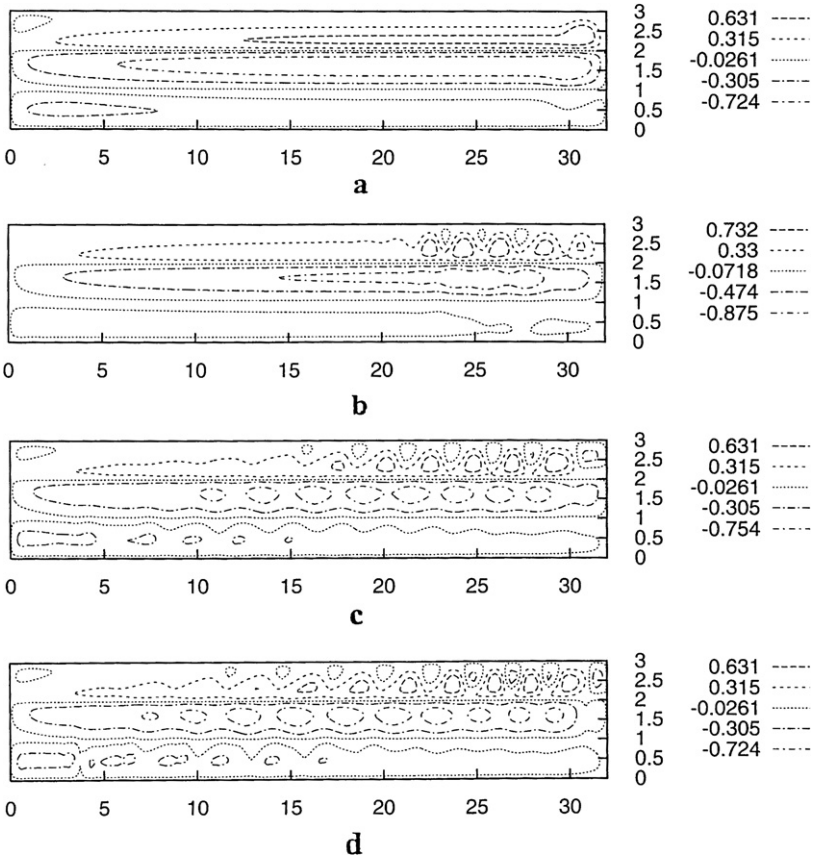

Fig. 10. Fields of (a)–(d) streamlines for the buoyant-thermocapillary motion at different moments of time ($G = 3825$, $M = 216\,000$, $L = 32$).

becomes unstable and one observes the oscillatory flow in the cavity (see Fig. 9). The vortices change their form and intensity during the oscillatory process.

Now let us consider the cavity with $L = 32$. As in the previous case, for sufficiently small values of M and G, the steady state takes place in the system. With the increase of G, the steady motion becomes unstable and one observes the transient process from the unicell structure (Fig. 10(a)) to the oscillatory multicell structure (Figs. 10(c), (d)). The chess-order configuration of vortices is obtained in the top layer. Since the thermocapillary effect plays the dominant role, the flow takes place mainly close to the interfaces.

5. Conclusion

The nonlinear thermocapillary and buoyant-thermocapillary flows in an asymmetric three-layer system, filling a closed cavity and subjected to a temperature gradient directed along the interfaces, are investigated. The shape and the amplitude of the convective flows are studied by the finite-difference method. For sufficiently large values of the Marangoni number, the steady state becomes unstable and the transient process takes place in the system: the long vortices break down and turn into the multicell structures. It is found that depending on G, the most intensive motion may be achieved in different layers. In the case of buoyant-thermocapillary flows the specific type of nonlinear oscillations, is obtained.

References

[1] I.B. Simanovskii, A.A. Nepomnyashchy, Convective Instabilities in Systems with Interface, Gordon and Breach, London, 1993.
[2] S. Wahal, A. Bose, Rayleigh-Benard and interfacial instabilities in two immiscible liquid layers, Phys. Fluids 31 (1988) 3502.
[3] A.A. Nepomnyashchy, I.B. Simanovskii, J.-C. Legros, Interfacial Convection in Multilayer Systems, Springer, New York, 2006.

[4] T. Doi, J.N. Koster, Thermocapillary convection in two immiscible layers with free surface, Phys. Fluids A 5 (1993) 1914.
[5] P. Georis, J.-C. Legros, Pure thermocapillary convection in multilayer system: first results from the IML-2 mission, in: L. Ratke, H. Walter, B. Feuerbacher (Eds.), Materials and Fluids under Low Gravity, Springer, Berlin, 1996, p. 299.
[6] H. Groothuis, F.G. Zuiderweg, Influence of mass transfer on coalescence of drops, Chem. Eng. Sci. 12 (1960) 288.
[7] I.B. Simanovskii, Anticonvective, steady and oscillatory mechanisms of instability in three-layer systems, Physica D 102 (1997) 313.
[8] A.A. Nepomnyashchy, I.B. Simanovskii, Combined action of different mechanisms of instability in multilayer systems, Phys. Rev. E 59 (1999) 6672.
[9] A. Prakash, D. Fujita, J.N. Koster, Surface tension and buoyancy effects on a free-free layer, Eur. J. Mech. B/Fluids 12 (1993) 15.
[10] A. Prakash, J.N. Koster, Natural and thermocapillary convection in three layers, Eur. J. Mech. B/Fluids 12 (1993) 635.
[11] A. Prakash, J.N. Koster, Convection in multiple layers of immiscible liquids in a shallow cavity. I. Steady natural convection, Int J. Multiphase Flow 20 (1994) 383.
[12] A. Prakash, J.N. Koster, Convection in multiple layers of immiscible liquids in a shallow cavity. II. Steady thermocapillary convection, Int J. Multiphase Flow 20 (1994) 397.
[13] I.B. Simanovskii, Thermocapillary flows in a three-layer system with a temperature gradient along the interfaces, Eur. J. Mech. B/Fluids 26 (2007) 422.
[14] I.B. Simanovskii, Nonlinear buoyant-thermocapillary flows in a three-layer system with a temperature gradient along the interfaces, Phys. Fluids 19 (2007) 082106.
[15] J. Priede, G. Gerbeth, Convective, absolute and global instabilities of thermocapillary-buoyancy convection in extended layers, Phys. Rev. E 56 (1997) 4187.
[16] V.M. Shevtsova, I.B. Simanovskii, A.A. Nepomnyashchy, J.-C. Legros, Thermocapillary convection in a symmetric three-layer system with the temperature gradient directed along the interfaces, C. R. Mecanique 333 (2005) 311.
[17] Ph. Georis, J.-C. Legros, A.A. Nepomnyashchy, I.B. Simanovskii, A. Viviani, Numerical simulation of convection flows in multilayer fluid systems, Microgravity Sci. Techn. 10 (1997) 13.
[18] P.G. Drazin, W.H. Reid, Hydrodynamic Stability, Cambridge University Press, Cambridge, 1981.